The phase diagram and thermodynamics of sodium fulleride from electrochemical measurements

1994 J. Phys.: Condens. Matter 6 5387

(http://iopscience.iop.org/0953-8984/6/28/013)

J. Phys.: Condens. Matter 6 (1994) 5387–5396. Printed in the UK

The phase diagram and thermodynamics of sodium fulleride from electrochemical measurements

Joon Hong Kim†, Anthony Petric†, P K Ummat‡ and W R Datars‡

† Department of Materials Science and Engineering, McMaster University, Hamilton, Ontario L8S 4L7, Canada

‡ Department of Physics and Astronomy, McMaster University, Hamilton, Ontario, L8S 4M1, Canada

Received 5 January 1994, in final form 24 January 1994

Abstract. Phase relations and thermodynamic properties of sodium fulleride (Na_xC_{60}) have been measured up to $x = 6$ by the electromotive force (EMF) method. Na β-alumina was used as the solid electrolyte and Na was added to the cell containing a fixed amount of fullerene by coulometric titration. The phase diagram is characterized by alternate single-phase regions (EMF varying with composition) and two-phase regions (EMF plateaus). At 599 K, the Gibbs energies of formation of Na_3C_{60} and Na_6C_{60} are 113.2 and 94.7 kJ/mole of Na, respectively. A model is proposed for the Na activity (or EMF) as a function of composition based on nearest-neighbour interactions, orientational disorder and a random distribution of Na ions. The ionic size and the hindrance of rotation of C_{60} accounts for the miscibility gap in alkali fullerides in this model.

1. Introduction

Pure C_{60} forms the 'molecular crystal', fullerite [1] wherein the molecules are cubic close packed and weakly bonded by van der Waals forces. Below 250 K, the molecules are orientationally ordered and fullerite has a simple cubic structure. Above 250 K, rotational modes become excited and this orientational disorder results in the higher-symmetry face-centred cubic (FCC) structure without the need for a diffusion-driven transformation. The deviation from isotropic random orientation of the C_{60} molecule presents evidence that the C_{60} molecule is not freely rotating at room temperature [2]. The calculation of the cubic crystal field based on the non-uniform charge distribution on a C_{60} molecule [3] shows the dependence of the crystal field potential, which exhibits an absolute and a secondary minimum at angles of 98° and 38°, respectively, anticlockwise around the [111] axis. However, the remarkable change in the Raman spectra at about 400 K indicates that structural change occurs and the intermolecular interaction for each C_{60} molecule is isotropic above 400 K [4].

C_{60} can form many M_xC_{60} compounds with various alkali metal electron donors. For M = K, Rb or Cs, three phases have been characterized by x-ray diffraction: face-centred cubic ($x = 3$, except Cs), body-centred tetragonal ($x = 4$), and body-centred cubic ($x = 6$) [5, 6]. The fourth stable compound with M_1C_{60} (M = K, Rb, Cs) shows a phase transformation around 333 K [7]. The high-temperature form is a rock salt structure in which only the octahedral sites are occupied. The low-temperature phase is not a cubic, but a rhombohedral structure. Unique to K_xC_{60} at $x \geqslant 1.4$, an FCC site-disordered lattice phase with random occupancy of tetrahedral and octahedral sites exists below 433 K [7].

0953-8984/94/285387+10$19.50

At room temperature, three FCC structures [6, 8] have been reported in the Na_xC_{60} system, identified as FCC I, II and III. Pure C_{60} has the FCC I structure with excitement of rotational motions (dynamic orientational disorder). Na intercalates into both tetrahedral and octahedral sites in this structure. Na_3C_{60} has the FCC II structure with full occupancy of every available tetrahedral and octahedral site by one Na atom. However, due to steric effects, rotation of C_{60} is hindered in this structure. The orientational disorder comes from merohedral disorder (random site-by-site population of two different standard orientations) [1]. Regardless of the type of disorder, both structures have an $Fm\bar{3}m$ symmetry. In the FCC III structure, the C_{60} molecules are orientationally ordered ($Fm\bar{3}$) with the tetrahedral sites occupied by one Na atom and the octahedral sites occupied by a cluster of four to nine Na atoms; a cluster of four Na atoms corresponds to Na_6C_{60} [8] and a cluster of nine Na atoms yields $Na_{11}C_{60}$ [9]. At room temperature Na_xC_{60} ($1 < x < 3$) is one phase with a simple cubic structure where the molecule has two preferred orientations as in low-temperature simple cubic pure C_{60} [10]. This phase transforms to the FCC structure with preferred occupancy of tetrahedral sites. The orientational transformation temperature is higher than in pure C_{60} (325 K for $x = 1.3$).

M_3C_{60} (FCC, M = K, Rb and mixed alkali metals) exhibits superconductivity [11] with an onset temperature comparable to or higher than those of traditional metallic superconductors. Unlike the complicated structure of copper oxide superconductors, the simple structure of alkali fullerides yields a monotonic relationship [12] between the superconducting transition temperature and the lattice parameter, which can be explained on the basis of conventional Bardeen–Cooper–Schrieffer (BCS) theory. This relationship suggests a T_c of approximately 15 K for Na_3C_{60}, which is isostructural with other superconducting alkali fullerides. However, no superconductivity has been observed above 2 K in Na_3C_{60}. As a possible explanation, the disproportionation of Na_3C_{60} [8] was proposed.

Due to slow reaction kinetics, the preparation of Na_xC_{60} is very difficult and different preparation methods may have resulted in different structures. No overall thermodynamic study on the Na–C_{60} system is known. In this work, we have measured the thermodynamic properties of Na_xC_{60} by an electrochemical technique, which provides more accurate control of composition and a more reliable preparation method.

Consideration of statistical mechanics can provide a useful tool in explaining the behaviour of these systems. We have modelled the phase changes in the Na–C_{60} system by the consideration of the orientational disorder of C_{60} molecules, random distribution of Na ions in interstitial sites and the nearest-neighbour interaction between Na ions and C_{60} molecules.

2. Experimental details

The usual preparation route was used to make C_{60}. Carbon soot was made by applying an electrical discharge between 6 mm graphite rods in a chamber containing He gas maintained at a pressure of 100 Torr. A mixture of C_{60} and C_{70} was obtained by using a soxhlet extractor with toluene as the solvent. After removing the solvent in a rotary evaporator, the C_{60} was separated from the mixture of fullerides by column chromatography with an eluent of hexane and 5% toluene. Finally the C_{60} was cleaned and purified by a sublimation method.

Dense Na β-alumina electrolyte tubes (> 98% density) were fabricated by conventional ceramic processes (slip casting and solid state sintering). Each tube was glass sealed to an α-alumina lid with a 3 mm diameter hole for inserting materials into the tube. An He

leak test was employed to select tubes with a good seal, i.e., those having a leak rate less than 10^{-8} cm^3 s^{-1}. After filling each cell with the working electrode or reference electrode component in an Ar atmosphere, a Ta cone was fixed to the α-alumina lid by a compression seal. This provided a hermetic closure for the cell as well as an electrical feedthrough. Thereafter, the experiment was operated in an Ar atmosphere glove box.

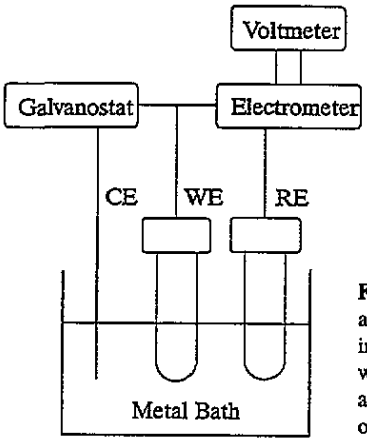

Figure 1. A schematic diagram of the EMF measurement apparatus. The WE and RE components were contained in closed Na β-alumina tubes. These WE and RE cells were immersed in the CE (the metal bath contained in a Ta crucible). The electrodes were connected to the outer circuit by Ta leads.

The experimental apparatus used for the electromotive force (EMF) measurements is shown in figure 1. The cell consisted of a reference electrode (RE), a counter electrode (CE), a working electrode (WE), which can be represented as

(RE) (CE) (WE)

$$\text{Ta|Bi–17 at.\% Na|Na } \beta\text{-alumina|Na–Pb–Bi|Na } \beta\text{-alumina|Na}_x\text{C}_{60}\text{|Ta}$$

where the RE (Bi–17 at.% Na) was calibrated against a pure Na electrode using a similar cell configuration. All EMF readings are reported with respect to the pure Na reference. The CE had a eutectic composition of Pb–Bi with a small amount of Na (< 1 wt%). The role of the CE was to provide a source of Na for coulometric titration and an electric contact between the RE and the CE. The WE was initially charged with about 50 mg of fullerene and 200 mg of Ni powder. Ni powder which is essentially unreactive to both Na and C, provided the electrical contact between the β-alumina and the Ta lead. The composition of the WE was changed in precise increments by coulometric titration at low current (< 0.1 mA). The total amount of charge was controlled to four significant digits. After each interval of coulometric titration, the galvanostat was switched off and the EMF was monitored by a chart recorder. At 675 K it took a few days to several weeks to stabilize the EMF. Equilibrium was verified by cycling the temperature between 475 and 725 K and checking that the EMF returned to the initial value.

Two sets of measurements were obtained at 599 K with different WE cells, the first with a raw C_{60}/C_{70} feedstock (9/1 ratio) and the second with pure C_{60}.

3. Results and discussion

The results of the EMF measurements are shown in figure 2. The electrochemical potential relates EMF, E, to the chemical activity of Na by the equation

$$E = -(RT/F)\ln a_{\text{Na}} \tag{1}$$

where R, T, F and a_{Na} are respectively the gas constant, absolute temperature, Faraday constant and chemical activity of Na in the WE with respect to pure Na. For dilute solutions, E obeys the Nernst law

$$E = E^0 - (RT/F) \ln X_{Na} \tag{2}$$

where the sodium atom fraction X_{Na} is calculated with respect to Na atoms and C_{60} molecules. (The C_{60} molecule is treated as an elementary unit in the solution since the covalent bonds between sixty C atoms remain intact throughout the ionization process.) Figure 3 shows this relation at 599 K. The theoretical value of the slope (RT/F) is 51.6 mV, and based on this, the best fit of E^0 is 950.3 mV. The solubility of Na in C_{60} is less than 1 mol.% ($\sim 0.7\%$) at 599 K.

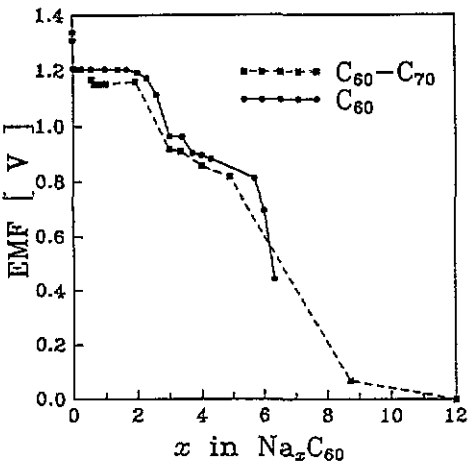

Figure 2. EMF versus x in Na_xC_{60} at 599 K. The squares are for a C_{60} and C_{70} mixture (9/1 ratio) and the circles are for pure C_{60}.

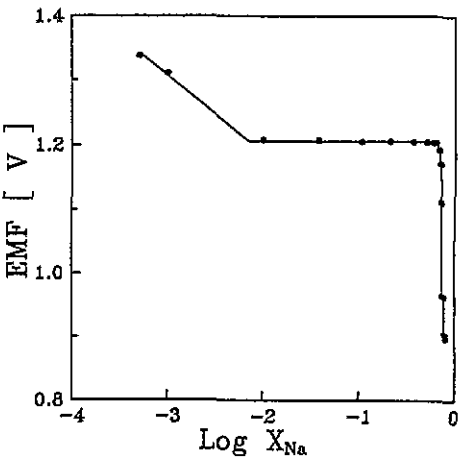

Figure 3. EMF versus $\log X_{Na}$ (at 599 K) shows Henrian behaviour in the dilute-solution region.

In figure 2, the large plateau in EMF ($0 < x < 1.7$) represents a two-phase region between FCC I and FCC II at 599 K. In the two-phase region the Na_xC_{60} in the WE is a mixture of $Na_{x_1}C_{60}$ and $Na_{x_2}C_{60}$ where $x_1 \simeq 0$ and $x_2 \simeq 1.7$. As the total amount of Na increases the ratio of the two phases changes. However, the chemical compositions of the two phases are fixed. Thus, the chemical activity of Na is constant in this region, whereas, in a single-phase region (solid solution region), the chemical activity of Na changes as a function of the composition. The region of gradual decrease in EMF ($1.7 < x < 3$) represents the domain of the FCC II phase. Another two-phase region ($3 < x < 3.3$) exists between FCC II and the following phase. The phase relations at higher concentrations ($x > 3.3$) have not been determined. A sudden drop in EMF in the range of $3.3 < x < 3.7$ leaves the possibility that a line phase may exist at some stoichiometry between 3.3 and 3.7. The FCC III structure forms a large solution region beyond $x = 3.7$ (or 3.3). The existence of Na atom clusters in the octahedral site suggests a range of compounds Na_xC_{60}, $3.7 < x < 11$. This is similar to Li_xC_{60} where a solution range $3 < x < 11$ has been observed [13]. However, it is possible that the FCC III phase has a miscibility gap: a lower-x phase with four Na atoms per cluster and a higher-x phase with nine Na atoms per cluster.

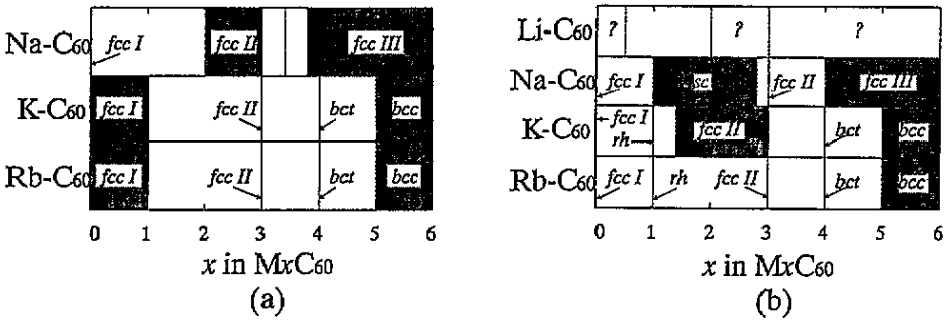

Figure 4. Proposed phase diagrams of alkali fullerides for (*a*) high temperatures (> 433 K) and (*b*) low temperatures (near room temperature). The Na_xC_{60} line phase may exist between $x = 3.3$ and $x = 3.7$ and is followed by the FCC III phase. The diagram for Cs fulleride is expected to be similar to that of Rb except at $x = 3$. Uncertain compounds and boundaries are represented by dashed lines.

The phases in alkali fullerides are listed in table 1. The proposed phase equilibria of several alkali–fullerene systems are shown in figure 4. Since the data from the literature are not in complete agreement, we have made arbitrary choices in some cases. It appears that the size of the alkali ion and the related orientational ordering of the C_{60} molecule are major factors in determining the phase relations. From equation (1), the activity of Na was calculated from the EMF data. The activity of C_{60} was derived by Gibbs–Duhem integration using the α function [15] (figure 5).

$$\alpha_i = (\ln \gamma_i)/(1 - X_i)^2 \tag{3}$$

$$\ln \gamma_2 = -\alpha_1 X_1 X_2 - \int_{x_2=1}^{x_2} \alpha_1 \, dX_2. \tag{4}$$

The Gibbs energy of mixing (ΔG_m) was calculated from the measured activity of Na (equation (1)) and the calculated activity of C_{60} (equation (4)) and is shown in figure 6. From the Gibbs energy of mixing, the Gibbs energies of formation of Na_3C_{60} and Na_6C_{60} are evaluated as 113.2 and 94.7 kJ mol^{-1} of Na, respectively.

We have attempted to model the Na–C_{60} system at high temperatures (> 400 K) by the use of statistical mechanics. The Gibbs energy, G, is expressed as

$$G = -kT \ln Q(N, V, T) \tag{5}$$

where k, N, V and Q are the Boltzmann constant, number of atoms or molecules, volume and canonical ensemble partition function, respectively.

If we consider the following reaction:

$$x\text{Na} + \text{C}_{60} = \text{Na}_x\text{C}_{60}(\text{FCC II}) \tag{6}$$

the Gibbs free energy of each species can be written as

$$xG^0_{\text{Na}} = -kT \ln(q_{\text{Na}})^{xN} + xNU_{\text{Na}} \tag{7}$$

$$G^0_{60} = -kT \ln(q_{60})^N + NU_{60} \tag{8}$$

$$G_x = -kT \ln(q'_{60})^N (q_t)^{N_1} (q_o)^{N_o} - kT \ln \Omega'(x) + NU_x \tag{9}$$

Table 1. The phases in alkali fullerides.

Composition		Structure	Temperature (K)	Remarks
C_{60}	$x = 0$	SC	$T < 260$	Orientationally ordered with two preferred orientations [1]
		FCC	$260 < T < 400$	Anisotropic dynamic disorder [2]
		FCC	$400 < T$	*Isotropic dynamic disorder [4]*
Li_xC_{60}	$x = 0.5, 2, 3$–11	FCC	$T = 353$	[13]
Na_xC_{60}	$1 < x < 3$	SC	$T < 325$	The orientational order is the same as in pure C_{60} (SC) [10]
		FCC	$325 < T < ?$	*[10]*
	$2 < x \leqslant 3$	FCC	$? < T$	Merohedral disorder [6, 8]
	$4 < x < 11$	FCC	$0 < T$	Ordered orientation; Na clusters [8, 9]
M_xC_{60}[a]	$x < 1$	FCC	$T = 300$	[14]
	$x = 1$	FCC	$330 < T$	Disordered orientation; rock salt structure [7]
		Rhombohedral	$T < 330$	[7]
	$1.4 < x < 3$	FCC	$? < T < 433$	Unique to K [7]
	$x = 3$	FCC	$0 < T$	Except Cs; merohedral disorder [5, 6, 14]
	$x = 4$	BCT	$0 < T$	[14]
	$x = 6$	BCC	$0 < T$	[14]

[a] M = K, Rb, Cs.

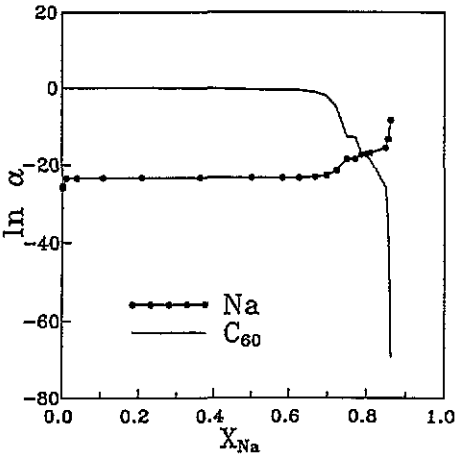

Figure 5. The activities of Na (measured) and C_{60} (calculated by Gibbs–Duhem integration) at 599 K.

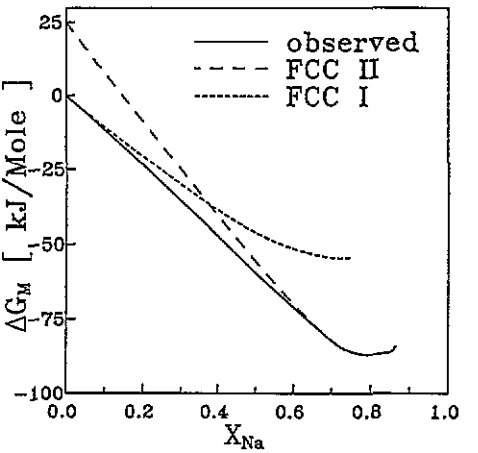

Figure 6. The Gibbs energy of mixing at 599 K. The curves for FCC I and II are from equations (22) and (12), respectively. The solid line is from $(X_A RT \ln a_A + X_B RT \ln a_B)$ where A and B represent Na and C_{60} and activities are calculated by equations (1) and (4).

where G^0_{Na} is the molar Gibbs energy of pure Na, G^0_{60} the molar Gibbs energy of pure C_{60}, G_x the Gibbs energy of Na_xC_{60}, q_{Na} the partition function of Na in pure Na, q_{60} the partition function of C_{60} in pure C_{60}, q'_{60} the partition function of C_{60} in Na_xC_{60}, q_t the partition function of Na at a tetrahedral site in Na_xC_{60}, q_o the partition function of Na at an octahedral site in Na_xC_{60}, N the number of C_{60} molecules, N_t the number of Na atoms at tetrahedral sites, N_o the number of Na atoms at octahedral sites, U_i the potential energy of each species and $\Omega'(x)$ the configurational term. Assuming that the difference of potential energy is given as

$$N(U_x - U_{60} - xU_{Na}) = N_t E_t + N_o E_o + Nax^2 \tag{10}$$

and that random distribution of Na atoms and merohedral disorder of C_{60} molecules gives the configurational term $\Omega'(x)$ where

$$\Omega'(x) = [2N!/N_t!(2N - N_t)!][N!/N_o!(N - N_o)!]2^N \tag{11}$$

and that q'_{60} is independent of x, then the Gibbs energy of mixing at constant temperature is given in the form of

$$\Delta G_m = N_t A + N_o B + Nax^2 + NC - kT \ln \Omega(x) \tag{12}$$

where

$$A = -kT \ln(q_t/q_{Na}) + E_t$$

$$B = -kT \ln(q_o/q_{Na}) + E_o$$

$$C = -kT \ln(q'_{60}/q_{60}) - kT \ln 2$$

$$\Omega(x) = [2N!/N_t!(2N - N_t)!]N!/N_o!(N - N_o)!.$$

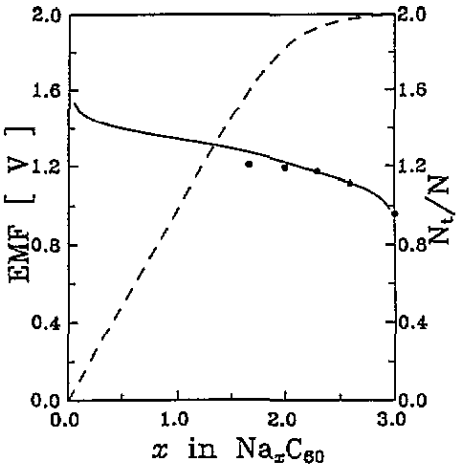

Figure 7. EMF and occupancy of tetrahedral sites: circles for measured EMF, solid line for the best fit of equation (12) and dashed line for the occupancy of tetrahedral sites in equation (15*b*).

Consider an equilibrium distribution of Na atoms between tetrahedral and octahedral sites. At constant pressure and temperature, the condition for equilibrium distribution of Na in Na_xC_{60} is given as

$$(\partial \Delta G_m/\partial N_t)_{P,T,N,x} = 0. \tag{13}$$

Define M as

$$M = \exp(-(A-B)/kT) = ([N_t/(2N-N_t)]/[N_o/(N-N_o)])_{\text{equilibrium}}. \tag{14}$$

Since $N_t + N_o = xN$, the equilibrium distribution is given, if $M = 1$, as

$$N_t/N = \tfrac{2}{3}x \tag{15a}$$

and otherwise as

$$N_t/N = \left[M(x+2) + 1 - x - \sqrt{[M(x+2)+1-x]^2 - 8M(M-1)x}\right]/2(M-1). \tag{15b}$$

The chemical activity of Na is defined as

$$(\partial \Delta G_m/\partial xN)_{P,T,N} = kT \ln a_{Na}. \tag{16}$$

Using equations (1), (12) and (14), equation (16) results in

$$-eE = A + kT \ln \frac{N_t/2N}{1-(N_t/2N)} + 2ax \tag{17a}$$

or

$$-eE = B + kT \ln \frac{N_o/N}{1-(N_o/N)} + 2ax \tag{17b}$$

where e is an elementary charge and (N_t/N) is given by equation (15).

We can determine the unknown parameters A, B and a for which equation (17) gives the best fit to the measured values. A plot of this relation, taking A, B and a as -1.34, -1.14 and 0 eV, where the value of a is chosen arbitrarily, is shown in figure 7. Note that in Na_2C_{60}, about 90% of tetrahedral sites are occupied; a higher occupancy of tetrahedral sites was experimentally observed at this composition [8, 10].

In order to complete equation (12), we need to determine the parameter C. The main difference between FCC I and FCC II originates from the type of orientational disorder in molecules. Assume that

$$-kT\ln(q'_{60}/q_{60}) = -kT\ln(q_{\text{lib}}/q_{\text{rot}}) \tag{18}$$

where q_{lib} and q_{rot} are the partition functions of rotational libration and free rotation, respectively (above 400 K, the rotational motion is almost isotropic [4]) and the changes in intramolecular and intermolecular vibrational frequencies are ignored. The rotational partition function [16] is given by

$$q_{\text{rot}} = (\pi^{1/2}/\sigma)(T/\Theta_{\text{r}})^{3/2} \tag{19a}$$

where

$$\Theta_{\text{r}} = h^2/8\pi^2 Ik. \tag{19b}$$

The symmetry number σ is 60 and the moment of inertia is 9.7×10^{-44} kg m^2, assuming a uniform shell with radius 0.35 nm. At 599 K the contribution of rotation to the Gibbs free energy is about -0.74 eV. The vibrational partition function [16] is given as

$$q_{\text{vib}} = \prod_i \exp(-h\nu_i/2kT)/[1-\exp(-h\nu_i/kT)]. \tag{20}$$

The librational frequencies of C_{60} molecules in pure C_{60} and K_3C_{60} were estimated as 24 cm^{-1} [17] and 26 cm^{-1} [18], respectively. Taking the frequency as 26 cm^{-1} the contribution of libration to the Gibbs free energy is about -0.44 eV. The contribution of merohedral disorder is about -0.036 eV. Thus the parameter C is about 0.26 eV. The resulting plot of equation (12) is shown in figure 6.

For the reaction, $x\text{Na} + C_{60} = \text{Na}_x\text{C}_{60}$ (FCC I), assuming that the number of C_{60} hindered in free rotation is proportional to the number of Na in interstitial sites, equation (12) is modified to

$$\Delta G_{\text{m}} = N_{\text{t}}A + N_{\text{o}}B + Nax^2 + (\alpha N_{\text{t}} + \beta N_{\text{o}})C - kT\ln\Omega(x) \tag{21}$$

where α and β are assumed to be constant in the dilute-solution region. Thus

$$\Delta G_{\text{m}} = N_{\text{t}}A' + N_{\text{o}}B' + Nax^2 - kT\ln\Omega(x) \tag{22}$$

where $A' = A + \alpha C$ and $B' = B + \beta C$. Note that A' and B' are less negative than A and B, respectively. α and β may be related to the steric effect and the contraction of the lattice parameter. Equation (22) is shown in figure 6 with $A' = -0.65$ and $B' = -0.95$ eV, which values are determined from figure 3, assuming $\alpha > \beta$.

The shift of miscibility gap from $0 < x < 2$ in Na_xC_{60} to $1 < x < 3$ in Rb_xC_{60} at room temperature can be explained by the preference of occupancy, which is related to A, B, α and β. When we consider the sizes of alkali ions and tetrahedral (~ 2.2 Å) and octahedral (~ 4 Å) sites, α should be much larger than β. In Na_xC_{60} (FCC II), because A is more negative than B and Na ions fill tetrahedral sites first, the initial slope of ΔG_{m} (FCC II) is determined by A and the ΔG_{m} (FCC II) curve is bent near $x = 2$ ($X_{\text{Na}} = 0.67$) in figure 6. However, in Na_xC_{60} (FCC I), the initial slope is determined by A' ($= A + \alpha C$) or B' ($= B + \beta C$); A' is less negative than A by 0.26α and B' is less negative than A by $B - A + 0.26\beta$. In either case, the initial slope of ΔG_{m} (FCC I) is much less steep than

that of ΔG_m (FCC II). Thus, Na_xC_{60} has a large miscibility gap between $0 < x < 2$. In Rb_xC_{60}, assuming that the initial slope of ΔG_m (FCC II) is determined by B and that of ΔG_m (FCC I) is determined by B' $(B + \beta C)$, if β is very small, the two curves are almost parallel in the dilute-solution region. However, the ΔG_m (FCC I) curve is bent at $x = 1$ $(X_{Na} = 0.5)$. Thus, a miscibility gap exists for $1 < x < 3$. Although a discrepancy between this model and the real system is inevitable due to oversimplification of the potential energy term (equation (10)), this model can explain the extent of phase stability between FCC I and FCC II, at least qualitatively.

4. Conclusions

Thermodynamic properties of Na_xC_{60} were measured. Solid solution regions were observed for $2 < x < 3$ and $x > 3.7$. At 599 K, the Gibbs energies of formation of Na_3C_{60} and Na_6C_{60} are 113.2 and 94.7 kJ/mole of Na, respectively. A simple model based on nearest-neighbour interactions, orientational disorder and random distribution of Na ions can adequately explain the phase relations in this system. The ionic size and the hindrance of rotation of C_{60} accounts for the shift of the miscibility gap in alkali fullerides in this model.

Acknowledgment

We wish to thank the Natural Sciences and Engineering Research Council of Canada for financial support.

References

[1] Heiney P A 1992 *J. Phys. Chem. Solids* **53** 1333
[2] Chow P C, Jiang X, Reiter G, Wochner P, Moss S C, Axe J D, Hanson J C and McMullan R K 1992 *Phys. Rev. Lett.* **16** 2943
[3] Lamoen D and Michel K H 1993 *Z. Phys.* B **92** 323
[4] Hamanaka Y, Nakashima S, Hangyo M, Shinohara H and Saito Y 1993 *Phys. Rev.* B **48** 8510
[5] Zhou O and Cox D E 1992 *J. Phys. Chem. Solids* **53** 1373
[6] Murphy D W, Rosseinsky M J, Fleming R M, Tycko R, Ramirez A P, Haddon R C, Siegrist T, Dabbagh G, Tully J C and Walstedt R E 1992 *J. Phys. Chem. Solids* **53** 1321
[7] Zhu Q, Zhou O, Fischer J E, McGhie A R, Romanow W J, Strongin R M, Cichy M A and Smith A B III 1993 *Phys. Rev.* B **47** 13948
[8] Rosseinsky M J, Murphy D W, Fleming R M, Tycko R, Ramirez A P, Siegrist T, Dabbagh G and Barrett S E 1992 *Nature* **356** 416
[9] Yildirim T, Zhou O, Fischer J E, Bykovetz N, Strongin R A, Cichy M A, Smith A B III, Lin C L and Jelinek R 1992 *Nature* **360** 568
[10] Yildirim T, Fischer J E, Harris A B, Stephens P W, Liu D, Brard L, Strongin R M and Smith A B III 1993 *Phys. Rev. Lett.* **71** 1383
[11] Schüter M, Lannoo M, Needels M, Baraff G A and Tomanek D 1992 *J. Phys. Chem. Solids* **53** 1473
[12] Fleming R M, Ramirez A P, Rosseinsky M J, Murphy D W, Haddon R C and Zahurak S M 1991 *Nature* **352** 787
[13] Chabre Y, Djurado D, Armand M, Romanow W R, Coustel N, McCauley J P Jr, Fischer J E and Smith A B III 1992 *J. Am. Chem. Soc.* **114** 764
[14] Zhu Q, Zhou O, Coustel N, Vaughan G B M, McCauley J P Jr, Romanow W J, Fischer J E and Smith A B III 1991 *Science* **254** 545
[15] Lupis C H P 1983 *Chemical Thermodynamics of Materials* (New York: Elsevier) p 165
[16] McQuarrie D A 1976 *Statistical Mechanics* (New York: Harper Collins) p 137
[17] Olson J R, Topp K A and Pohl R O 1993 *Science* **259** 1145
[18] Belosludov V R and Shpakov V P 1992 *Mod. Phys. Lett.* B **6** 1209